Choline PET for Monitoring Early Tumor Response to Photodynamic Therapy

Baowei Fei[1], Hesheng Wang[2], Chunying Wu[3], and Song-mao Chiu[4]

[1]Department of Radiology, Emory Center for Systems Imaging, Emory University, Atlanta, Georgia; [2]Department of Biomedical Engineering, Case Western Reserve University, Cleveland, Ohio; [3]Department of Radiology, Case Western Reserve University, Cleveland, Ohio; and [4]Department of Radiation Oncology, Case Western Reserve University, Cleveland, Ohio

Photodynamic therapy (PDT) is a relatively new therapy that has shown promise for treating various cancers in both preclinical and clinical studies. The present study evaluated the potential use of PET with radiolabeled choline to monitor early tumor response to PDT in animal models. **Methods:** Two human prostate cancer models (PC-3 and CWR22) were studied in athymic nude mice. A second-generation photosensitizer, phthalocyanine 4 (Pc 4), was delivered to each animal by a tail vein injection 48 h before laser illumination. Small-animal PET images with ^{11}C-choline were acquired before PDT and at 1, 24, and 48 h after PDT. Time–activity curves of ^{11}C-choline uptake were analyzed before and after PDT. The percentage of the injected dose per gram of tissue was quantified for both treated and control tumors at each time point. In addition, Pc 4-PDT was performed in cell cultures. Cell viability and ^{11}C-choline uptake in PDT-treated and control cells were measured. **Results:** For treated tumors, normalized ^{11}C-choline uptake decreased significantly 24 and 48 h after PDT, compared with the same tumors before PDT ($P < 0.001$). For the control tumors, normalized ^{11}C-choline uptake increased significantly. For mice with CWR22 tumors, the prostate-specific antigen level decreased 24 and 48 h after PDT. Pc 4-PDT in cell culture showed that the treated tumor cells, compared with the control cells, had less than 50% ^{11}C-choline activity at 5, 30, and 45 min after PDT, whereas the cell viability test showed that the treated cells were viable longer than 7 h after PDT. **Conclusion:** PET with ^{11}C-choline is sensitive for detecting early changes associated with Pc 4-PDT in mouse models of human prostate cancer. Choline PET has the potential to determine whether a PDT-treated tumor responds to treatment within 48 h after therapy.

Key Words: small-animal PET; choline molecular imaging; photodynamic therapy (PDT); prostate cancer; tumor response

Photodynamic therapy (PDT) is a relatively new therapy that has shown promise for treating various cancers in both preclinical and clinical studies (1). PDT requires a photosensitizing drug, low-power laser light of an appropriate wavelength, and oxygen. On absorption of photons, the photosensitizer generates singlet oxygen and other reactive oxygen species that are toxic to cells (2). Various photosensitizing drugs have been synthesized for treating cancers in both animals and human patients (3–7). Noninvasive approaches for monitoring PDT effects are now needed to improve drug development and optimize treatment.

PET is noninvasive, and it is widely used in oncologic applications. PET with ^{18}F-FDG is routinely used to assess tumor response to therapy in cancer patients. Small-animal PET with ^{18}F-FDG has been used to monitor changes in glucose uptake after PDT in animals, as reported by us (8,9) and others (10,11). A decrease of ^{18}F-FDG uptake was observed in treated tumors after PDT. Other imaging tracers, such as radiolabeled annexin V, have been developed for imaging PDT-induced apoptosis (12,13).

In this study, we evaluated a second-generation PDT drug, phthalocyanine 4 (Pc 4), and explored the potential use of PET to study tumor response to Pc 4-PDT. Pc 4 has been evaluated for treating various human cancers and is currently undergoing clinical trials (3). Pc 4 localizes at the mitochondria, and photodynamic damage to cell membranes occurs immediately after PDT (14). On the other hand, choline is taken up into cells via a choline transporter, then metabolized to generate phosphocholine, and finally transferred to diacylglycerol to generate phosphatidyl choline, which is a major constituent of membrane lipids (Kennedy pathway) (15). In cancer cells, membrane synthesis is activated during cell proliferation, and the phosphocholine level is elevated (16–18). Malignant tumors show an increased uptake of choline, as documented in the literature (18). Robust overexpression of choline kinase has been found in most primary tumors (19), providing the basis for imaging cancer using choline PET (20) and choline MR spectroscopy (21). Both choline and the photosensitizer Pc 4 are related to cell membranes, possibly providing a rationale for the evaluation of choline PET as a means of detecting changes in tumor choline uptake after Pc 4-PDT. Although choline PET has been reported as a means of detecting various cancers including prostate cancer (22), it has not been used to monitor PDT and tumor response. Here, we report our choline studies for Pc 4-PDT

both in vivo and in vitro and discuss the potential clinical applications.

MATERIALS AND METHODS

Photosensitizer

Pc 4 [HOSiPcOSi(CH$_3$)$_2$(CH$_2$)$_3$N(CH$_3$)$_2$] was synthesized and characterized in the laboratory of Malcolm Kenney at Case Western Reserve University, using a previously detailed method (23). A stock solution (1 mg/mL) was made by dissolving Pc 4 in 50% Cremophor EL (Sigma-Aldrich) and 50% absolute ethanol and then adding 9 volumes of normal saline with mixing. For injection, the Pc 4 stock solution was mixed with an equal volume of 5% Cremophor EL, 5% ethanol, and 90% saline to give a final concentration of 0.05 mg/mL (0.07 mM).

Animal Tumor Models

The study was conducted with the approval of the Institutional Animal Care and Use Committee of Case Western Reserve University and conformed to the guidelines of the National Institutes of Health for the care and use of laboratory animals. Two human prostate cancer models (CWR22 and PC-3) were studied in the animals. Male athymic nude mice (age, 4–6 wk; weight, between 25 and 30 g) were obtained from the Case Comprehensive Cancer Center Athymic Animal Facility (Case Western Reserve University) and were housed 1 mouse/cage under pathogen-free conditions. They were maintained under controlled conditions (12-h dark–light cycles; temperature, $20°-24°C$), with free access to sterilized mouse chow.

The CWR22 xenograft model of human, androgen-dependent prostate cancer was maintained as previously described (24). A cell suspension containing approximately 1×10^7 cells in 0.2 mL of Matrigel (Collaborative Research) was injected subcutaneously through a 19-gauge needle into the rear flank of male, athymic, nude mice. Mice with CWR22 were given 12.5-mg sustained-release testosterone pellets (Innovative Research of America) subcutaneously before receiving tumor cells and at intervals of 3 mo until their death. For this CWR22 tumor model, only 1 tumor was initiated on each mouse; these animals were used to measure prostate-specific antigen (PSA) after treatment, to independently monitor therapeutic effect.

The PC-3 cell line was derived from a primary, malignant, human prostate tumor (25). PC-3 cells were grown as monolayers in Eagle's minimum essential medium supplemented with 15% fetal bovine serum at 37°C. Cells were harvested by trypsinization in ethylenediaminetetraacetic acid/trypsin, washed in Hank's balanced salt solution (HBSS) without Ca^{2+} and Mg^{2+}, and centrifuged at 150g for 5 min. Cells were counted in a hemacytometer with 0.4% trypan blue, and the cell suspension was brought to a final concentration of 1×10^6 viable cells/mL and kept on ice for immediate injection. For this tumor cell line, 2 tumors were initiated in each mouse by subcutaneous injection of 50 μL containing 5×10^4 PC-3 cells on each flank at least 20 mm apart and as far from the lung and heart as possible to minimize motion effects on PET.

PDT Protocol

Tumors were treated when the shortest dimension of the tumor reached 4–5 mm, which typically occurred 2–4 wk after implantation. Each animal was weighed at the time of injection, and a volume of Pc 4 solution was injected into the tail vein to give a drug dose of 0.6 mg/kg of body weight (e.g., 240 μL to a 20-g mouse). Forty-eight hours after the photosensitizer injection, the animals were taken to the small-animal imaging facility for imaging and PDT. A diode laser (Applied Optronics Corp.) delivered 672-nm light to the tumor surface, the longest wavelength absorption maximum of Pc 4. The laser was coupled to a fiberoptic cable terminating in a microlens. The treatment light covered the entire tumor and was uniformly distributed throughout the treatment field. The tumor on each animal was irradiated with a fluence of 150 J/cm^2 and an irradiance of 100 mW/cm^2, which have been shown to produce a complete response and some cures in PC-3 tumors (26). For the PC-3 tumor model, the second tumor in each animal served as a control (receiving photosensitizer but no light).

In this study, 15 mice were treated, among which 8 had PC-3 tumors and 7 had CWR22 tumors. For the PC-3 model, each mouse had 2 tumors, one of which was randomly selected for treatment and the other served as the control. The 2 tumors were approximately the same size when PDT was performed. For the CWR22 study, each mouse had only 1 tumor because the PSA levels were measured as an independent parameter to determine the treatment effect.

Radiosynthesis of ^{11}C-Choline

The synthesis method for ^{11}C-choline was previously reported (27). ^{11}C-carbon dioxide was produced by a Scanditronix MC17 cyclotron and was then bubbled into a reaction vial previously filled with LiAlH$_4$ in a tetrahydrofuran solution (0.1 mol/L, 1 mL) at room temperature. After the tetrahydrofuran was completely evaporated, hydriodic acid (57%, 1 mL) was added, and the reaction vial was heated to 120°C. ^{11}C-CH$_3$I obtained by this wet chemistry was then distilled, dried, and trapped onto an Accell Plus CM Sep-Pak cartridge that had been previously loaded with precursor N,N-dimethylaminoethanol (60 μL), which was at room temperature. The methylation reaction took place immediately. The final product was eluted from the cartridge by saline after being washed with ethanol and water and then passed through a 0.2-μm sterile filter. The radiolabeling yield was approximately 80% (corrected to ^{11}C-CH$_3$I). The radiochemical purity was greater than 99%, as determined by high-performance liquid chromatography (Partisil SCX cation exchange column, 250 mM NaH$_2$PO$_4$/CH$_3$CN [9:1, v/v]; flow rate, 1.8 mL/min).

PET Studies

Two days before PDT (day -2), the animal was injected with the photosensitizing drug Pc 4. Forty-eight hours later, the animal was taken to the small-animal PET facility for baseline image acquisition on day 0, immediately before laser irradiation for PDT. The first group of mice ($n = 4$) underwent an additional PET scan 1 h after PDT. Because the ^{11}C has a half-life of 20 min, there was a 4-h ($>$10 times of half-life) interval between the first and second PET scans. The second group of mice ($n = 5$) was scanned 24 h after PDT. The third group ($n = 6$) was imaged 48 h after PDT. Because our study focuses on detecting early tumor response to PDT, the mice were imaged no more than 2 d after PDT. A dedicated microPET imaging system (R4; Siemens Preclinical Solutions) was used in this study. Approximately 18.5 MBq of ^{11}C-choline in 0.1 mL of physiologic saline were injected into each animal via the tail vein. The mice were then immediately scanned for 60 min with a list-mode acquisition that allowed retrospective determination of time binning of dynamic data. During each imaging session, the animals were taped onto a plastic holder and were provided with a continuous supply of 2%

isoflurane (EZAnesthesia) in air. Animal respiration rates were monitored throughout the entire experiment; typically, the respiration rate was maintained at 40/min.

The PET emission scans were reconstructed using an ordered-subset expectation maximum reconstruction algorithm. Dynamic PET data were rebinned into 7 frames (600, 600, 600, 600, 600, 300, and 300 s). The dimension of the reconstructed volume was $128 \times 128 \times 63$ voxels. The interpolated pixel size of the PET images was 0.8×0.8 mm with a slice thickness of 1.2 mm.

Quantitative Image Analysis

The percentage of the injected dose per gram of tissue (%ID/g) was obtained using the Acquisition Sinogram and Image Processing software package installed with the microPET system and our in-house software. The %ID/g was calculated as the measured activity per unit of volume (calibrated in kBq/mL) divided by the injection dose (kBq) $\times$ 1 mL/g $\times$ 100. From the 7 frames of reconstructed PET images, normalized uptake values were calculated to generate normalized time–activity curves. The localization of the ^{11}C-choline accumulation on the PET images in relationship to the anatomic structures was aided by the visual comparison of the PET images with the transmission images. Each tumor was manually segmented on each image slice using the PET image. A 3-dimensional region of interest was drawn around the tumor regions. A separate 3-dimensional region of interest was used for each time point because the tumor size tended to change 24–48 h after treatment.

To quantify the tumor response in terms of the change of ^{11}C-choline uptake, the %ID/g response was calculated as a percentage change as indicated below:

$$\%ID/g \text{ response} = \left(\frac{\%ID/g_{dayn} - \%ID/g_{day0}}{\%ID/g_{day0}} \right) \times 100.$$

Histopathology

All tumors were stained with hematoxylin and eosin for the histopathologic assessment of the tumor features. To verify the histologic tumor responses to Pc 4-PDT, mice were euthanized 24 or 48 h after PDT. For the CWR22 mice, the tumors were harvested 24 ($n = 5$) and 48 h ($n = 2$) after PDT. For the PC-3 mice, 16 tumors (8 PDT-treated, 8 controls) were dissected 1 ($n = 8$) and 48 h ($n = 8$) after PDT. Dissected tumors were sliced into 2–3 slices, and excised tissues were fixed overnight in a large volume of 10% formalin. Histology slides were prepared at the Case Comprehensive Cancer Center Histology Core Facility. Tissue sections of the entire specimen were then examined with an Olympus BX40 microscope at magnifications ranging from $\times$40 to $\times$400.

In Vitro PDT in Cell Culture

Pc 4-PDT was performed in cells, and choline uptake was measured at various time points after PDT. PC-3 cells were cultured in RPMI 1640 medium in 3 wells of 6-well plates at a concentration of $2–3 \times 10^5$ cells per well. Half of the plates served as controls and the other half was treated with PDT (200 nM of Pc 4, 200 mW/cm^2, 200 mJ/cm^2). Immediately after PDT, culture medium was replaced with HBSS supplemented with 10 mM N-(2-hydroxyethyl)piperazine-N'-(2-ethanesulfonic acid) (pH 7.3) and 2% glucose because RPMI medium contains choline cholide. ^{11}C-choline (0.5 MBq) was loaded into each well, and the cultures were incubated at 37°C for 5, 30, and 45 min, respectively. After incubation, the medium was removed from the wells, and the cells were washed twice with 2 mL of HBSS, lysed with 2 mL of 1% Sarkosyl NL-97 (ICN), and then washed again with HBSS. The radioactivity in the incubation medium, lysates, and all of the washes was then determined separately using a 1282 Compu-gamma γ-well counter (Wallac, Inc.). Each procedure was carefully planned and timed during the experiment. All measured radioactivity was corrected for decay.

Cell Viability Test

After PDT, the viability of the cell populations was estimated using the trypan blue dye exclusion test (28) because the dye stains only the nonviable cells that have lost their plasma membrane integrity.

PC-3 cells were grown on glass cover slips in P60 dishes. Half of the plates served as controls and the other half was treated with PDT. At various times after receiving PDT, cell cultures were stained in situ for 10 min with 0.4% trypan blue solution at room temperature. The stained and unstained cells were then counted under a light microscope at $\times$20 magnification. At least 200 cells were randomly counted to determine the cell viability after each treatment because viable cells with membrane integrity were capable of trypan blue dye exclusion and thus remained unstained. Nonviable cells with compromised membrane integrity were incapable of trypan blue dye exclusion and were, therefore, stained. Cell viability was determined as the percentage of the ratio of the number of stained cells (nonviable) to the total number of unstained (viable) and stained (nonviable) cells.

Statistical Analysis

Statistical analyses were performed to compare the ^{11}C-choline uptake values obtained at 4 different time points (before PDT and at 1, 24, and 48 h after PDT). The mean and SD of the uptake values at 7 different time frames were calculated for the treated tumors. Similar analysis was performed for the control tumors. Furthermore, the difference between the pre-PDT and post-PDT uptake values was also analyzed for both treated and control tumors. We used Excel 2007 (Microsoft) to compute a 2-tailed, 2-sample Student t test. A P value less than or equal to 0.05 was assigned statistical significance.

RESULTS

Treated Tumors Responded to Therapy Within 48 h After Pc 4-PDT

Figure 1 shows photographs taken of a tumor-bearing mouse before PDT and at 1 d and 1 mo after PDT. One day after treatment, the mouse picture shows that the tumor rapidly responded to the therapy. Within 2 wk after treatment, the tumor shrank. One month after PDT, the tumor was healed, as shown in the picture. The mouse was monitored for 300 d, during which the tumor did not recur.

Table 1 shows that the PSA values of the 2 treated mice decreased at 24 and 48 h after PDT, further indicating the tumor response to Pc 4-PDT. The 2 mice (M1 and M2) were imaged and treated at the same time. Forty-eight hours after PDT, visible change of tumor tissue was observed in both mice. Tumor tissue demonstrated a greater change on mouse M2 than on mouse M1. Although the PSA values decreased in both mice, the decrease in PSA was greater in
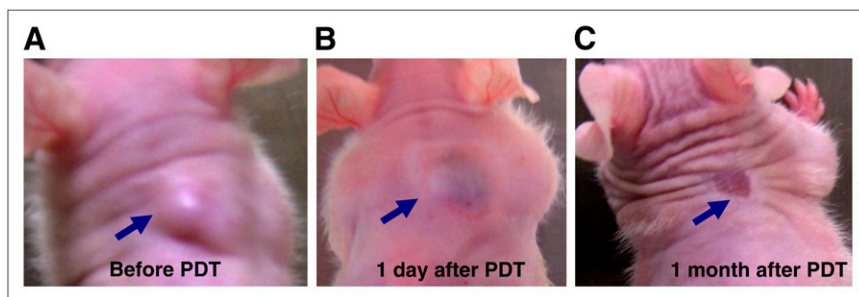
mouse M2, which had a higher PSA level (66.6 ng/mL) than did mouse M1 (44.6 ng/mL) before treatment. However, 2 d after PDT, both mice had similar PSA levels (28.1 ng/mL for mouse M1 and 29.3 ng/mL for mouse M2). The choline uptake decreased 48 h after PDT, compared with the pre-PDT values, in both mice (Table 1), but the decrease was greater in mouse M2. For mouse M1, the normalized uptake values (%ID/g) were 12.5 and 9.5 before therapy and 48 h after PDT, respectively. Therefore, the uptake decreased by 24.1% 48 h after PDT. For mouse M2, the mean uptake values were 19.0 and 7.8 before therapy and 48 h after PDT, respectively. The uptake decreased by 59.2% 48 h after PDT. The choline uptake was consistent with both changes of PSA level. This observation is encouraging because the change in choline uptake may be able to predict therapeutic effect on PDT-treated tumors.

^{11}C-Choline Uptake Decreased in Treated Tumors and Increased in Control Tumors at 48, 24, and 1 h After PDT

Figure 2 shows the small-animal PET images of a tumor-bearing mouse before PDT and 48 h after PDT. The mouse was implanted with 2 PC-3 tumors. One tumor was treated, and the other served as the control (which received Pc 4 but no light). Forty-eight hours after PDT, the PET images showed that the ^{11}C-choline activity within the PDT-treated tumor decreased. The PET images also showed high activity in the kidneys, which is consistent with other reports on ^{11}C-choline PET of animals. Compared with the treated

tumors, the control tumor showed slightly increased ^{11}C-choline activity and an increased tumor size due to the tumor growth during the 2 d.

Figure 3 shows the time–activity curves of ^{11}C-choline uptake in PC-3 tumors before PDT and 48 h after PDT. The %ID/g at the 7 frames (5, 15, 25, 35, 45, 53, and 57 min) was 17.7 ± 0.2 (mean ± SD) and 10.9 ± 0.1, respectively, immediately before therapy and 48 h after PDT. Therefore, the uptake by the treated tumors decreased by 38.4% 48 h after PDT ($P < 0.001$). In contrast, ^{11}C-choline uptake by the control tumors was increased at the 48-h time point. For the 4 untreated tumors from the same 4 mice, the normalized uptakes were 19.5 ± 2.0 and 26.3 ± 1.3 immediately before PDT and 48 h after PDT, respectively. Therefore, the ^{11}C-choline uptake by the untreated tumors increased by 35.0% during 2 d ($P < 0.001$). The increase in the choline uptake may have been caused by tumor growth, as suggested by the increase in tumor size.

Table 2 shows the ^{11}C-choline activity of the treated and control tumors for each mouse. A decrease in ^{11}C-choline uptake was observed in all of the treated tumors 48 h after therapy. The average %ID/g response was −37.8% for the 4 treated tumors. In contrast, an increase in ^{11}C-choline uptake was observed in all of the control tumors 48 h after therapy. The average %ID/g response was 34.6% for the 4 control tumors. Histologic images (Fig. 4) show the dramatic difference between the treated and control tumors 48 h after PDT in that there were massive areas of inflammation and damage within the treated tumor, although the untreated tumor was not damaged and the cells were intact.

This PET study was repeated in another mouse model (CWR22). Once again, the choline uptake was decreased at 48 h after PDT, as shown in Table 1 ($n = 2$). The average uptake of the PDT-treated tumors was 15.7 and 8.6 immediately before therapy and at 48 h after PDT, respectively. In this group, the uptake by the treated tumors was decreased by 45.3% 48 h after PDT.

To test other time points for imaging, we repeated the PET experiment 24 h after PDT ($n = 5$). The choline uptake for each mouse is listed in Table 3. For the 5 PDT-treated CWR22 tumors, the normalized uptake (%ID/g) was 17.4 ± 1.9 and 4.3 ± 0.4 immediately before therapy and 24 h after PDT, respectively. Therefore, the uptake by the treated tumors was decreased by 75.5% 24 h after PDT

TABLE 1. PSA Values (ng/mL) of Treated Mice and ^{11}C-Choline Uptake of Treated Tumors (CWR22) Before PDT and 48 Hours After PDT

	Mouse ID	
Parameter	M1	M2
PSA		
Before	44.6	66.6
24 h	34.8	41.8
48 h	28.1	29.3
%ID/g		
Before	12.5 ± 1.5	19.0 ± 1.9
48 h	9.5 ± 1.8	7.8 ± 1.3
%ID/g response	−24.1%	−59.2%

Uptake was measured by %ID/g. Numbers are means ± SDs of measurements at 7 frames (5, 15, 25, 35, 45, 53, and 57 min).
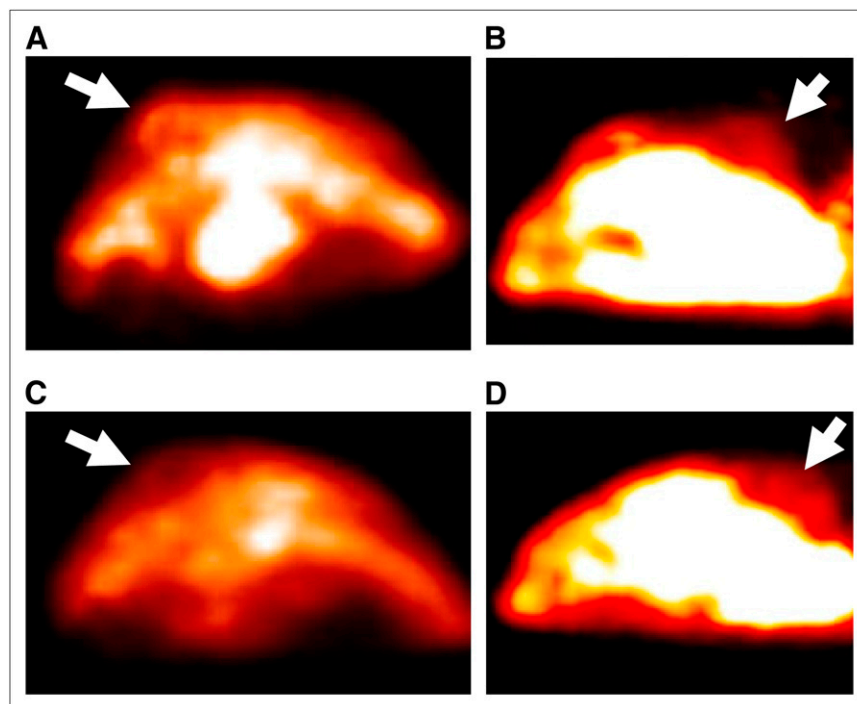
FIGURE 2. Transverse small-animal PET images of 2 PC-3 tumors (arrows). Images of treated tumor before PDT (A) and 48 h after PDT (C) show that ^{11}C-choline uptake of treated tumor had decreased 48 h after PDT. Images of control tumor before PDT (B) and 48 h after PDT (D) show slightly increased ^{11}C-choline uptake 48 h after PDT. Quantitative analysis results of ^{11}C-choline uptake in treated and control tumors confirmed our visual inspection; these results are shown in Figure 3.

($P < 0.001$). The 24-h group showed a greater decrease than did the 48-h group, suggesting we should image the animals at an even earlier time.

Table 4 shows the PET analysis results 1 h after PDT. Each mouse had 1 treated and 1 untreated tumor. The treated tumors had less choline uptake 1 h after therapy than did the pre-PDT tumors. The average %ID/g response was −27.7% for the 4 treated tumors just 1 h after PDT. Rapid tumor responses to Pc 4-PDT included acute edema and inflammation immediately after the treatment. However, the control tumors, except that in mouse M15, showed slightly increased choline uptake 1 h after therapy. For the 4 untreated tumors from the same 4 mice, the average uptake was 20.7 and 22.7 at baseline and 1 h later, respectively.

^{11}C-Choline Uptake of PDT-Treated Tumor Cells Decreased Within 45 min After Treatment, but Cells Were Viable Within 7 h After PDT

To separate the effect of the in vivo tissue microenvironment from that of cellular activity, we studied the effect of PDT on the uptake of ^{11}C-choline in cultured PC-3 cells. As shown in Figure 5, the choline uptake of cultured cells decreased at all 3 time points (5, 30, and 45 min after PDT) by more than 50% (56.2% ± 6.0%) in the treated cells, compared with the control cells. There was only a small SD at each time point (5% ± 2%). The uptake rate of ^{11}C-choline in the treated cells is only 46% of that in the control cells. The choline uptake of the treated cells decreased immediately (5 min) after PDT.

To further examine the viability of the treated cells, the trypan blue test was performed after PDT at different time points (30, 45, 60, and 450 min). Table 5 shows that the PDT-treated cells were still viable within 60 min after therapy. The percentage of nonviable cells was less than 3% at 60 min after PDT, which is within the same range as control cells without PDT (Table 5). More than 90% of the PDT-treated cells were still viable even 450 min after treatment. This viability result was consistent with those of our early in vitro studies with Pc 4-PDT of various types of cancer cells.
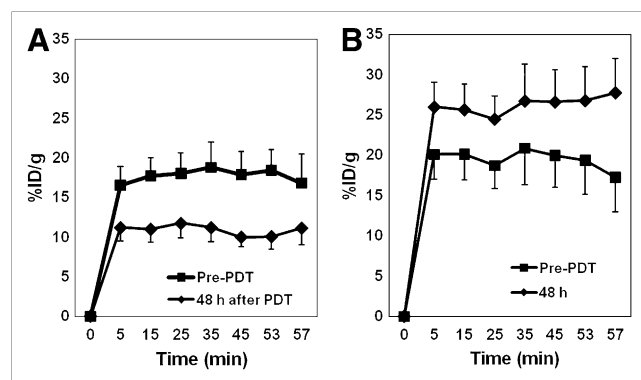

FIGURE 3. Time–activity curves of ^{11}C-choline in PDT-treated PC-3 tumors ($n = 4$) (A) and in control tumors ($n = 4$) (B) of same mice before PDT and 48 h after PDT. Uptake of ^{11}C-choline was measured as %ID/g. Error bars represent SEs.

DISCUSSION

The PET technique can be used to noninvasively monitor early tumor response to PDT and thus has the potential to optimize PDT in preclinical and clinical studies. PET may

TABLE 2. ¹¹C-Choline Uptake of PDT-Treated and Control Tumors (PC-3) Before PDT and 48 Hours After PDT

Parameter	Mouse ID			
	M3	M4	M5	M6
Treated tumors				
Before	10.2 ± 0.9	21.2 ± 1.8	22.2 ± 1.6	17.3 ± 2.6
48 h	6.4 ± 0.4	12.2 ± 2.3	13.0 ± 1.6	12.1 ± 1.5
%ID/g response	−37.3%	−42.5%	−41.5%	−30.0%
Control tumors				
Before	12.9 ± 0.5	22.5 ± 1.3	23.1 ± 3.2	19.5 ± 1.7
48 h	17.0 ± 0.4	27.5 ± 2.5	34.4 ± 3.6	26.3 ± 2.2
%ID/g response	32.3%	22.3%	48.8%	34.9%

Numbers are %ID/g. Means ± SDs of %ID/g were calculated at 7 frames (5, 15, 25, 35, 45, 53, and 57 min). Each mouse (M3–M6) had 2 tumors; one was treated and other served as control.

also be used to design and optimize the treatment for each patient. If a patient does not have an early response, alternative treatments can then be initiated and the patient can be spared the potential morbidity resulting from delayed treatment. We recently demonstrated the promise of Pc 4-PDT for treating human prostate cancer in an animal model (26). It has also been demonstrated in animal models that Pc 4-PDT is effective for treating human breast cancer (29), human ovarian epithelial carcinoma (30), human colon cancer (31), and human glioma (32). The National Cancer Institute's Drug Decision Network sponsored preclinical toxicity and pharmacokinetic evaluations of Pc 4 and developed a formulation appropriate for its use in humans (33). Pc 4-PDT is under 2 phase I clinical trials for treating patients with cutaneous T-cell lymphoma (3), ensuring the ability to translate this animal PET study to human patients for monitoring PDT in clinical settings because all major hospitals have PET scanners.
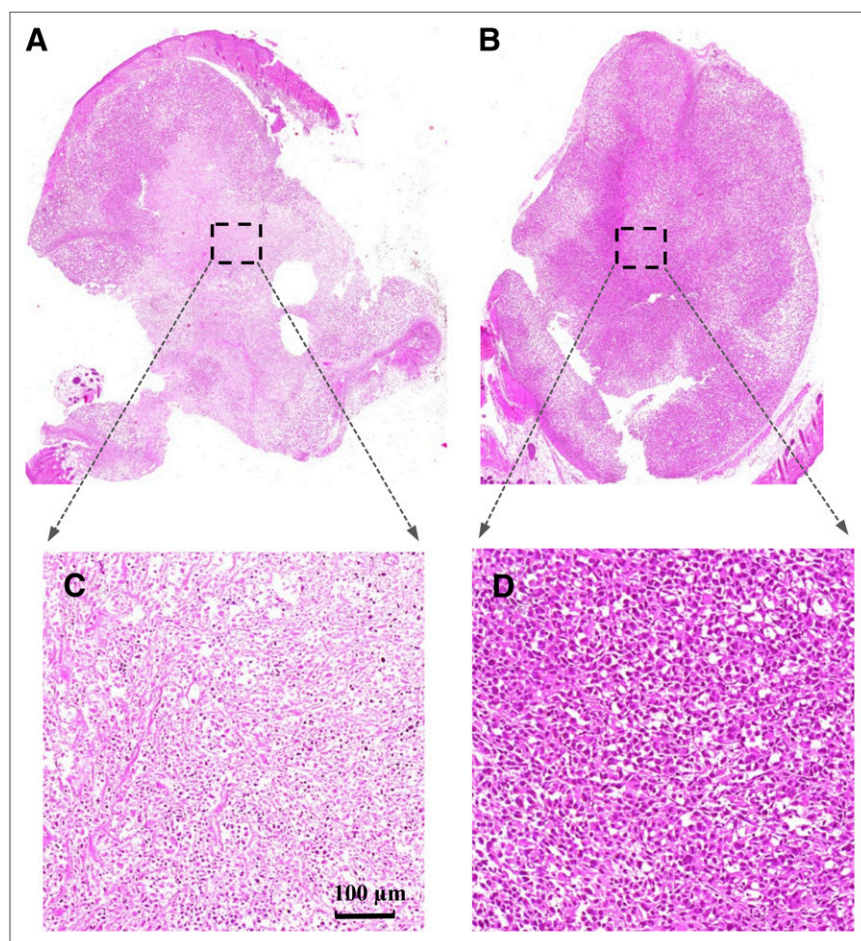

FIGURE 4. Histologic images of treated and control PC-3 tumors at 48 h after PDT. Inflammatory response with edema was observed in treated tumor (A) but was not seen in control tumor (B). Rectangular areas on A and B are magnified and shown in C and D, respectively. In C, massive areas of treated tissue were damaged by PDT; however, control tumor cells remained intact (D).

TABLE 3. PSA Values (ng/mL) of PDT-Treated Mice and ^{11}C-Choline Uptake of Treated Tumors (CWR22) Before PDT and 24 Hours After PDT

	Mouse ID				
Parameter	M7	M8	M9	M10	M11
PSA					
Before	27.4	48.4	20.4	43.6	NA
24 h	26.4	34.5	14.3	35.5	NA
%ID/g					
Before	16.2 ± 3.6	14.2 ± 2.4	15.1 ± 3.8	17.7 ± 1.7	23.6 ± 2.3
24 h	1.0 ± 0.2	4.6 ± 0.3	7.2 ± 1.1	4.2 ± 0.8	4.2 ± 1.0
%ID/g response	−94.1%	−67.3%	−52.2%	−76.0%	−82.0%

Uptake was measured as %ID/g. Numbers are means ± SDs at 7 frames (5, 15, 25, 35, 45, 53, and 57 min). PSA was not available (NA) for mouse M11.

Choline PET may offer a new approach for PDT monitoring and tumor response assessment. Previous studies for monitoring PDT have focused on measuring the light dose, oxygen level, or drug concentration. Light dosimetry is critically important for limiting the light dose delivered to vulnerable areas of normal tissue (34). Other studies have monitored the hemoglobin oxygen levels (35) and the local blood flow (36). Various methods have also been developed to measure tissue photosensitizer levels (37). Because PDT requires 3 components—that is, drug, light, and oxygen—any of them can be the limiting factor in determining the PDT effect in a target tumor. The overall amount of light delivered to a tumor is not a reliable predictor of the PDT effect (38); however, monitoring all 3 parameters and the interplay of the factors in tissue can be complicated. Furthermore, invasive monitoring approaches can limit their clinical applications. Because choline PET is noninvasive and can provide functional information regarding tumor response to the therapy, it may be used to monitor the treatment and assess the therapeutic efficacy.

The PDT-induced decrease of choline uptake represents the early tumor response to PDT, which can be explained by the observations of previous in vitro mechanism studies. Extensive, early Pc 4-PDT studies in cell cultures have identified cardiolipin and the antiapoptotic proteins Bcl-2 and Bcl-xL as targets of Pc 4-PDT; the intrinsic pathway of apoptosis, with the key participation of caspase-3, as the central response of many human cancer cells to Pc 4-PDT; and signaling pathways that could modify apoptosis (3). It has been shown that Pc 4 exhibits mitochondrial localization and binds at or near cardiolipin (39). Cardiolipin is a phospholipid that comprises approximately 22% by weight of the inner membrane lipid of mitochondria and participates in membrane bilayers (40). It has been shown that Pc 4-PDT has profound effects on cellular membranes (14). Mitochondrial reactive oxygen species were detected within minutes of cell exposure to Pc 4 and to photo-activating light, followed by mitochondrial inner membrane permeabilization, depolarization and swelling, cytochrome c release, and apoptotic cell death. On the other hand, choline is a substrate for the synthesis of phosphocholine, a precursor of phosphatidylcholine (a major constituent of membrane phospholipids), including cardiolipin (Kennedy pathway) (15). In cancer cells, membrane synthesis is activated during cell proliferation and the phosphocholine level is elevated (16). Pc 4-PDT reduces choline uptake as measured in both cell cultures and animals and may, thus, represent an early tumor response to the therapy. As demonstrated in this study, the early tumor response is detectable by small-animal PET with radiolabeled choline.

TABLE 4. ^{11}C-Choline Uptake of Treated and Control Tumors (PC-3) Before PDT and 1 Hour After PDT

	Mouse ID			
Parameter	M12	M13	M14	M15
Treated tumors				
Before	11.9 ± 1.3	13.6 ± 1.9	24.9 ± 2.9	23.3 ± 3.8
1 h	11.0 ± 0.7	8.5 ± 1.2	14.7 ± 3.0	17.6 ± 3.0
%ID/g response	−8.1%	−37.3%	−41.0%	−24.4%
Control tumors				
Before	14.7 ± 1.9	19.4 ± 2.7	21.2 ± 2.9	27.4 ± 5.3
1 h	16.4 ± 1.0	23.9 ± 1.9	26.6 ± 1.3	23.7 ± 1.2
%ID/g response	11.6%	23.2%	25.8%	−13.3%

Numbers represent %ID/g and %ID/g response. Means ± SDs were calculated from 7 frames (5, 15, 25, 35, 45, 53, and 57 min).
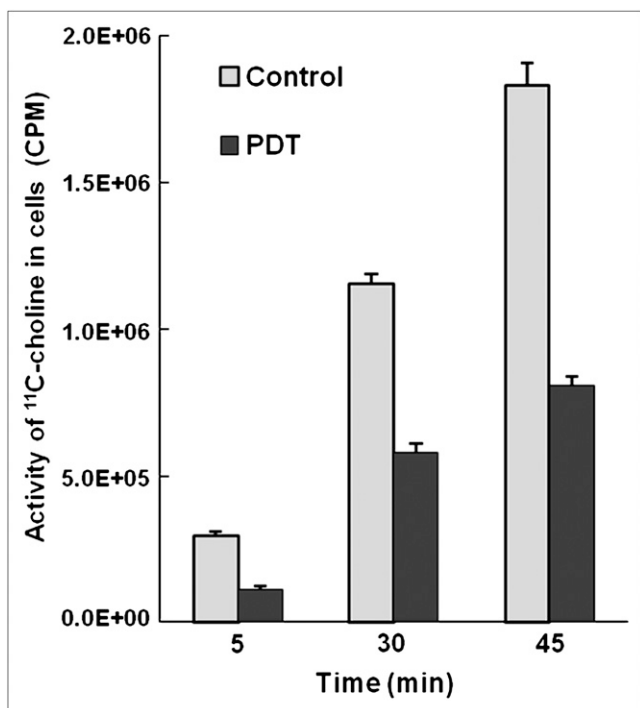
FIGURE 5. Pc 4-PDT–induced changes in ^{11}C-choline uptake as function of post-PDT incubation time (5, 30, and 45 min). Activity of ^{11}C-choline in PC-3 cells was measured by γ-counter, and unit was counted per minute (CPM). Each data point represents 3 wells of cells, and error bars are SD.

The in vivo PET findings were consistent with change in PSA level and histology. Choline PET is particularly useful for androgen-independent prostate tumors such as the PC-3 model when PSA is not available as a biomarker for the

TABLE 5. Cell Viability Test at Various Times After PDT					
Time after PDT (min)	Dish no.	Total	Viable	Nonviable	Nonviable %
30	1	200	193	7	3.5%
	2	200	198	2	1.0%
	3	200	196	4	2.0%
45	4	224	217	7	3.1%
	5	235	225	10	4.3%
	6	452	430	22	4.9%
60	7	208	203	5	2.4%
	8	250	244	6	2.4%
	9	273	268	5	1.8%
450	10	227	210	17	7.5%
	11	230	212	18	7.8%
	12	213	193	20	9.4%
No PDT450	13	211	207	4	1.9%
	14	322	315	7	2.2%
	15	203	198	5	2.5%

Cell cultures were stained with trypan blue solution. Unstained (viable) and stained (nonviable) cells were counted for each dish (nos. 1–15). Percentages of nonviable cells were calculated for both treated and control dishes.

evaluation of treatment response. The choline PET technique may be able to assess the response of other types of tumors to the therapy. To the best of our knowledge, this represents the first reported study demonstrating the usefulness of PET with radiolabeled choline for detecting early tumor response to PDT.

Caution should be used when applying the conclusion from our data to other studies. Although we used 2 human prostate cancer models (PC-3 and CWR22), the tumors were implanted in athymic mice, which do not show the expected immune response of a human patient. Results from tumor xenografts in mice may not extrapolate directly to human cancers. In this study, we did not evaluate the tumors for more than 2 d after PDT because we focused on the early tumor response to PDT. It is likely that the timing of posttherapy imaging will be an important factor in the usefulness of PET for monitoring the therapeutic response. In this study, ^{11}C-choline, rather than ^{18}F-labeled choline analogs, was used for the PET experiments because the ^{11}C-choline tracer can provide information regarding the natural choline, both in vivo and in vitro. ^{11}C has a shorter half-life than does ^{18}F. In another study, we are currently investigating the possible use of MRI to quantify tumor necrosis and the change of blood flow after PDT; this may give a useful, further insight into the PDT mechanism. In this preliminary study, our results indicate that in animal models, in vivo PET with radiolabeled choline may be able to reveal early tumor response to PDT within 48 h after treatment.

CONCLUSION

We evaluated small-animal PET with ^{11}C-choline as a potential, noninvasive imaging marker for monitoring tumor response to PDT in mice. PET images are able to reveal PDT-induced changes in ^{11}C-choline uptake of treated tumors from 1 to 48 h after therapy. Treated tumors demonstrated a marked decrease of choline uptake after treatment, whereas increases in ^{11}C-choline uptake were observed in untreated tumors at the same time. Histologic images verified the therapeutic effect on the treated tumors. PET with radiolabeled choline may provide a noninvasive tool for monitoring early tumor response to PDT, evaluating new PDT drugs, optimizing PDT, and assessing the therapeutic efficacy of PDT.

REFERENCES

1. Triesscheijn M, Baas P, Schellens JH, Stewart FA. Photodynamic therapy in oncology. *Oncologist.* 2006;11:1034–1044.
2. Oleinick NL, Morris RL, Belichenko I. The role of apoptosis in response to photodynamic therapy: what, where, why, and how. *Photochem Photobiol Sci.* 2002;1:1–21.
3. Miller JD, Baron ED, Scull H, et al. Photodynamic therapy with the phthalocyanine photosensitizer Pc 4: the case experience with preclinical mechanistic and early clinical-translational studies. *Toxicol Appl Pharmacol.* 2007;224: 290–299.
4. Weersink RA, Bogaards A, Gertner M, et al. Techniques for delivery and monitoring of TOOKAD (WST09)-mediated photodynamic therapy of the prostate: clinical experience and practicalities. *J Photochem Photobiol B.* 2005; 79:211–222.
5. Zaak D, Sroka R, Stocker S, et al. Photodynamic therapy of prostate cancer by means of 5-aminolevulinic acid-induced protoporphyrin IX: in vivo experiments on the dunning rat tumor model. *Urol Int.* 2004;72:196–202.
6. Moore CM, Nathan TR, Lees WR, et al. Photodynamic therapy using meso tetra hydroxy phenyl chlorin (mTHPC) in early prostate cancer. *Lasers Surg Med.* 2006;38:356–363.
7. Du KL, Mick R, Busch TM, et al. Preliminary results of interstitial motexafin lutetium-mediated PDT for prostate cancer. *Lasers Surg Med.* 2006;38:427–434.
8. Fei B, Wang H, Muzic RF Jr, et al. Deformable and rigid registration of MRI and microPET images for photodynamic therapy of cancer in mice. *Med Phys.* 2006;33:753–760.
9. Fei B, Muzic R, Lee Z, et al. Registration of micro-PET and high resolution MR images of mice for monitoring photodynamic therapy. *Proc SPIE.* 2004;5369: 371–379.
10. Lapointe D, Brasseur N, Cadorette J, et al. High-resolution PET imaging for in vivo monitoring of tumor response after photodynamic therapy in mice. *J Nucl Med.* 1999;40:876–882.
11. Berard V, Rousseau JA, Cadorette J, et al. Dynamic imaging of transient metabolic processes by small-animal PET for the evaluation of photosensitizers in photodynamic therapy of cancer. *J Nucl Med.* 2006;47:1119–1126.
12. Subbarayan M, Hafeli UO, Feyes DK, Unnithan J, Emancipator SN, Mukhtar H. A simplified method for preparation of ^{99m}Tc-annexin V and its biologic evaluation for in vivo imaging of apoptosis after photodynamic therapy. *J Nucl Med.* 2003;44:650–656.
13. Cauchon N, Langlois R, Rousseau JA, et al. PET imaging of apoptosis with ^{64}Cu-labeled streptavidin following pretargeting of phosphatidylserine with biotinylated annexin-V. *Eur J Nucl Med Mol Imaging.* 2007;34:247–258.
14. Lam M, Oleinick NL, Nieminen AL. Photodynamic therapy-induced apoptosis in epidermoid carcinoma cells: reactive oxygen species and mitochondrial inner membrane permeabilization. *J Biol Chem.* 2001;276:47379–47386.
15. Kennedy EP, Weiss SB. The function of cytidine coenzymes in the biosynthesis of phospholipides. *J Biol Chem.* 1956;222:193–214.
16. Glunde K, Jacobs MA, Bhujwalla ZM. Choline metabolism in cancer: implications for diagnosis and therapy. *Expert Rev Mol Diagn.* 2006;6:821–829.
17. Katz-Brull R, Margalit R, Degani H. Differential routing of choline in implanted breast cancer and normal organs. *Magn Reson Med.* 2001;46:31–38.
18. Yoshimoto M, Waki A, Obata A, Furukawa T, Yonekura Y, Fujibayashi Y. Radiolabeled choline as a proliferation marker: comparison with radiolabeled acetate. *Nucl Med Biol.* 2004;31:859–865.
19. Lenkinski RE, Bloch BN, Liu F, et al. An illustration of the potential for mapping MRI/MRS parameters with genetic over-expression profiles in human prostate cancer. *MAGMA.* 2008;21:411–421.
20. DeGrado TR, Baldwin SW, Wang S, et al. Synthesis and evaluation of ^{18}F-labeled choline analogs as oncologic PET tracers. *J Nucl Med.* 2001;42:1805–1814.
21. Gillies RJ, Morse DL. In vivo magnetic resonance spectroscopy in cancer. *Annu Rev Biomed Eng.* 2005;7:287–326.
22. DeGrado TR, Coleman RE, Wang S, et al. Synthesis and evaluation of ^{18}F-labeled choline as an oncologic tracer for positron emission tomography: initial findings in prostate cancer. *Cancer Res.* 2001;61:110–117.
23. Oleinick NL, Antunez AR, Clay ME, Rihter BD, Kenney ME. New phthalocyanine photosensitizers for photodynamic therapy. *Photochem Photobiol.* 1993;57:242–247.
24. Pretlow TG, Delmoro CM, Dilley GG, Spadafora CG, Pretlow TP. Transplantation of human prostatic carcinoma into nude mice in Matrigel. *Cancer Res.* 1991;51:3814–3817.
25. Kaighn ME, Narayan KS, Ohnuki Y, Lechner JF, Jones LW. Establishment and characterization of a human prostatic carcinoma cell line (PC-3). *Invest Urol.* 1979;17:16–23.
26. Fei B, Wang H, Meyers J, Feyes D, Oleinick NL, Duerk JL. High-field magnetic resonance imaging of the response of human prostate cancer to Pc4-based photodynamic therapy in an animal model. *Lasers Surg Med.* 2007;39:723–730.
27. Pascali C, Bogni A, Itawa R, Cambiè M, Bombardieri E. [^{11}C]Methylation on a C18 Sep-Pak cartridge: a convenient way to produce [N-methyl-^{11}C]choline. *J Labelled Comp Radiopharm.* 2000;43:195–203.
28. Ray SK, Karmakar S, Nowak MW, Banik NL. Inhibition of calpain and caspase-3 prevented apoptosis and preserved electrophysiological properties of voltage-gated and ligand-gated ion channels in rat primary cortical neurons exposed to glutamate. *Neuroscience.* 2006;139:577–595.
29. Whitacre CM, Satoh TH, Xue L, Gordon NH, Oleinick NL. Photodynamic therapy of human breast cancer xenografts lacking caspase-3. *Cancer Lett.* 2002;179: 43–49.
30. Colussi VC, Feyes DK, Mulvihill JW, et al. Phthalocyanine 4 (Pc 4) photodynamic therapy of human OVCAR-3 tumor xenografts. *Photochem Photobiol.* 1999;69: 236–241.
31. Whitacre CM, Feyes DK, Satoh T, et al. Photodynamic therapy with the phthalocyanine photosensitizer Pc 4 of SW480 human colon cancer xenografts in athymic mice. *Clin Cancer Res.* 2000;6:2021–2027.
32. George JE, Ahmad Y, Varghai D, et al. Pc 4 photodynamic therapy of U87-derived human glioma in the nude rat. *Lasers Surg Med.* 2005;36:383–389.
33. Egorin MJ, Zuhowski EG, Sentz DL, Dobson JM, Callery PS, Eiseman JL. Plasma pharmacokinetics and tissue distribution in CD2F1 mice of Pc4 (NSC 676418), a silicone phthalocyanine photodynamic sensitizing agent. *Cancer Chemother Pharmacol.* 1999;44:283–294.
34. Zhu TC, Finlay JC, Hahn SM. Determination of the distribution of light, optical properties, drug concentration, and tissue oxygenation in-vivo in human prostate during motexafin lutetium-mediated photodynamic therapy. *J Photochem Photobiol B.* 2005;79:231–241.
35. Yu G, Durduran T, Zhou C, et al. Noninvasive monitoring of murine tumor blood flow during and after photodynamic therapy provides early assessment of therapeutic efficacy. *Clin Cancer Res.* 2005;11:3543–3552.
36. Li H, Standish BA, Mariampillai A, et al. Feasibility of interstitial Doppler optical coherence tomography for in vivo detection of microvascular changes during photodynamic therapy. *Lasers Surg Med.* 2006;38:754–761.
37. Zhou X, Pogue BW, Chen B, et al. Pretreatment photosensitizer dosimetry reduces variation in tumor response. *Int J Radiat Oncol Biol Phys.* 2006;64:1211–1220.
38. Sterenborg H, de Wolf J, Koning M, Kruijt B, van den Heuvel A, Robinson D. Phosphorescence-fluorescence ratio imaging for monitoring the oxygen status during photodynamic therapy. *Opt Express.* 2004;12:1873–1878.
39. Morris RL, Azizuddin K, Lam M, et al. Fluorescence resonance energy transfer reveals a binding site of a photosensitizer for photodynamic therapy. *Cancer Res.* 2003;63:5194–5197.
40. Hoch FL. Cardiolipins and biomembrane function. *Biochim Biophys Acta.* 1992; 1113:71–133.

Fei BW, Wang H, Wu C, Chiu SM. Choline PET for monitoring early tumor response to photodynamic therapy. Journal of Nuclear Medicine 2010; 51:130-138.

This paper is publically available in the PubMed Central

http://www.ncbi.nlm.nih.gov/pubmed/20008981